OCL 2016, 23(1) D113
© B.R. Hopiavuori *et al.*, Published by EDP Sciences 2015
DOI: 10.1051/ocl/2015056

OCL Oilseeds & fats Crops and Lipids
Available online at:
www.ocl-journal.org

Review – Dossier Open Access

Lipids and brain
Lipides et cerveau

Very long-chain fatty acids support synaptic structure and function in the mammalian retina

Blake R. Hopiavuori[1,2,⋆], Lea D. Bennett[5], Richard S. Brush[2,4], Matthew J. Van Hook[6], Wallace B. Thoreson[6,7] and Robert E. Anderson[1–4]

[1] Oklahoma Center for Neuroscience, University of Oklahoma Health Sciences Center, 608 S. L. Young Boulevard, Oklahoma City, OK 73104 Oklahoma, USA
[2] Dean McGee Eye Institute, Oklahoma City, Oklahoma, USA
[3] Department of Cell Biology, University of Oklahoma Health Sciences Center, Oklahoma City, Oklahoma, USA
[4] Department of Ophthalmology, University of Oklahoma Health Sciences Center, Oklahoma City, Oklahoma, USA
[5] Retina Foundation of the Southwest, Dallas, Texas, USA
[6] Department of Ophthalmology and Visual Sciences, University of Nebraska Medical Center, Omaha, Nebraska, USA
[7] Department of Pharmacology and Experimental Neuroscience, University of Nebraska Medical Center, Omaha, Nebraska, USA

Received 7 June 2015 – Accepted 15 June 2015

Abstract – Elongation of Very Long chain fatty acids-like 4 (ELOVL4) is a fatty acid elongase responsible for the biosynthesis of very long chain (VLC; ≥ C26) fatty acids in the retina, brain, skin, Meibomian gland, and testes. Heterozygous inheritance of mutant *ELOVL4* causes juvenile macular degeneration in autosomal dominant Stargardt-like macular dystrophy (STGD3). Retinal photoreceptors are enriched with VLC polyunsaturated fatty acids (VLC-PUFAs), which have been shown by our group and others to be necessary for the survival of rod photoreceptors. Our group performed a series of studies using mice conditionally depleted of retinal *Elovl4* (KO) aimed at understanding the role of VLC-PUFAs in long-term retinal health and function, focusing on the role of these fatty acids in mediating synaptic function between the photoreceptors and the rest of the neural retina. The absence of VLC-PUFA from the retina of KO mice resulted in a marked decrease in retinal b-wave responses of the electroretinogram as well as a decrease in the amplitude of the oscillatory potentials mediated by the neural retina. Although there were no measureable differences between KO and wild type (WT) mice in either pre-synaptic rod calcium channel function or post-synaptic bipolar cell glutamate receptor responses, ultrastructural analysis revealed a marked decrease in the diameter of synaptic vesicles in rod terminals. Recent quantification suggests that this decrease in synaptic vesicle size due to the absence of VLC-PUFAs in KO mice, and the consequent decrease in glutamate content, could account for the decrease in b-wave response amplitudes that were previously measured in these animals.

Keywords: ELOVL4 / very long chain fatty acids / very long chain polyunsaturated fatty acids / Stargardt-like macular dystrophy / Lipids in retinal structure and function

Résumé – Les acides gras à très longue chaîne participent à la structure et à la fonction synaptique dans la rétine des mammifères. L'ELOVL4 (elongation of very long chain fatty acids-like 4) est une élongase d'acide gras impliquée spécifiquement dans la voie de biosynthèse d'acides gras à très longue chaîne (VLC de longueur de chaîne ≥ 26 atomes de carbone) dans la rétine, le cerveau, la peau, la glande de Meibomius (glande sébacée située dans l'épiderme des paupières) et les testicules. La transmission de la mutation hétérozygote *ELOVL4* provoque une dégénérescence maculaire juvénile dans la dystrophie maculaire autosomique dominante de type Stargardt (STGD3). Les photorécepteurs rétiniens sont enrichis en acides gras polyinsaturés à très longue chaîne (AGPI-VLC), qui s'avèrent nécessaires à la survie des photorécepteurs en bâtonnet. Afin de mieux comprendre le rôle spécifique de ces acides gras dans le fonctionnement rétinien et à plus long terme la santé, notre groupe de recherche a effectué une série d'études utilisant des souris génétiquement dépourvues (KO) en ELOVL4 rétinienne, en se concentrant sur la médiation de la fonction synaptique entre les photorécepteurs et le reste de la rétine neurale. L'absence d'AGPI-VLC dans la rétine de la souris KO pour ELOVL4 conduit à une diminution marquée de la réponse électrique de sa rétine, à savoir ondes b de l'électrorétinogramme et amplitude des potentiels oscillatoires véhiculés par la rétine neurale.

⋆ Correspondence: blake-hopiavuori@ouhsc.edu

Bien qu'il n'y ait pas de différences mesurables entre les souris KO et sauvage au niveau des fonctions présynaptique des cellules en bâtonnet (canaux calciques) et postsynaptique des cellules bipolaires (récepteurs au glutamate), une analyse ultrastructurale a révélé une diminution marquée du diamètre des vésicules synaptiques au niveau terminal (bâtonnets). Une donnée récente suggère que cette diminution de la taille des vésicules synaptiques chez la souris KO pour ELOVL4 déficiente en AGPI-VLC, et la diminution consécutive du contenu du glutamate, pourrait expliquer la diminution des amplitudes de réponse des ondes b qui ont été précédemment mesurée chez ces animaux.

Mots clés : Acides gras à très longue chaîne / acides gras polyinsaturés à très longue chaîne / dystrophie maculaire de type Stargardt / lipides dans la structure et la fonction rétinienne

1 Introduction

Elongation of Very Long chain fatty acids-like 4 (ELOVL4) is a fatty acid elongase responsible for the biosynthesis of very long chain (VLC; ≥ C26) fatty acids that are found as components of more complex lipid molecules such as sphingolipids and phospholipids in the retina, brain, skin, Meibomian gland, and testes (Agbaga *et al.*, 2008; Aveldano, 1987; Brush *et al.*, 2010; Poulos *et al.*, 1987; Vasireddy *et al.*, 2007). In the retina the predominant VLC fatty acids are polyunsaturated fatty acids (VLC-PUFA) which are typically esterified within a phosphatidylcholine molecule alongside DHA (22:6 n3) (Agbaga *et al.*, 2010) (Fig. 1). VLC saturated fatty acids (VLC-SFA) are primarily found in sphingolipids (Brush *et al.*, 2010; Poulos, 1995).

Autosomal dominant Stargardt-like macular dystrophy (STGD3) is a juvenile form of progressive macular degeneration that begins with onset of vision loss as early as nine years of age and is characterized by loss of the macula and subsequent formation of a central scotoma. STGD3 is caused by a five base pair deletion and frameshift mutation in exon six of the *ELOVL4* gene (Donoso *et al.*, 2001; Edwards *et al.*, 2001; Griesinger *et al.*, 2000; Kniazeva *et al.*, 1999; Zhang *et al.*, 2001). The frameshift mutation induces a pre-mature stop codon and causes a premature termination of the transcript, resulting in a truncated ELOVL4 protein devoid of its ER-retention motif. Since the ELOVL4 protein must be retained in the ER to perform its enzymatic function (Agbaga *et al.*, 2008; Barabas *et al.*, 2013; Harkewicz *et al.*, 2012; Logan *et al.*, 2014), loss of the ER-retention motif causes the ELOVL4 protein to be mislocalized within the cytosol (Agbaga *et al.*, 2014). The mutant protein does not have any enzymatic activity of its own (Logan *et al.*, 2013). However, using *in vitro* cell-based and cell-free microsomal assays, we found that co-expression of different forms of both wild-type and mutant ELOVL4 resulted in a significant dominant-negative effect of the mutant protein on both localization and enzymatic activity of the wild-type protein (Logan *et al.*, 2013). This suggests that the retina phenotype observed in STGD3 results from a loss of VLC-PUFA products due to the dominant negative effect of an enzymatically inactive mutant protein.

It is known that VLC-PUFA are incorporated into phosphatidylcholine and are densely packed into photoreceptor outer segment membranes, but their presence and function in retinal synapses was relatively unknown until recently. To determine the role of VLC-PUFA in the structure and function of retinal synapses, we conditionally deleted *Elovl4* from rod and cone photoreceptors in mice and evaluated inner retinal function, synaptic architecture, and the ultrastructure of VLC-PUFA-depleted photoreceptor terminals (Bennett *et al.*, 2014).

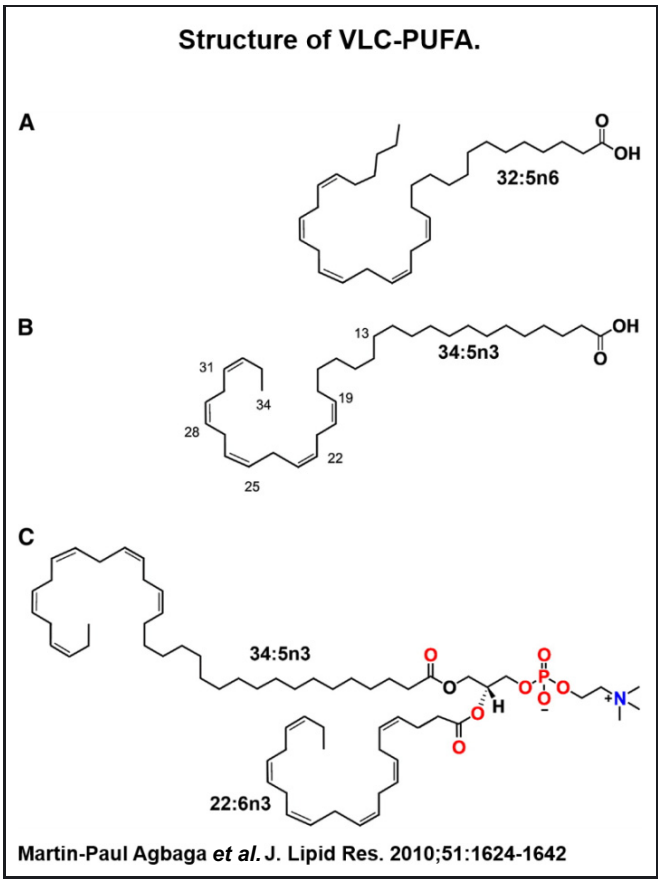

Fig. 1. Structure of VLC-PUFA. Free FA form of VLC-PUFA 32:5 n6 (A) and 34:5 n3 (B). Note the polyunsaturated methyl end and the saturated carboxyl terminal ends. (C) A typical phospholipid containing VLC-PUFA esterified to the *sn-1*position of the glycerol backbone. LC-PUFA, either 22:6 n3 or 20:4 n6, or others can occupy the *sn-2* position. The *sn-3* position in this scenario is occupied by phosphocholine (This research was originally published in *Journal of Lipid Research*. Agbaga *et al.*, Retinal very long-chain PUFAs: new insights from studies on ELOVL4 (2010). © The American Society for Biochemistry and Molecular Biology).

2 Retinal synapses contain VLC-PUFA

Ribbon and conventional synapses were prepared from fresh bovine retinas by sucrose gradient centrifugation

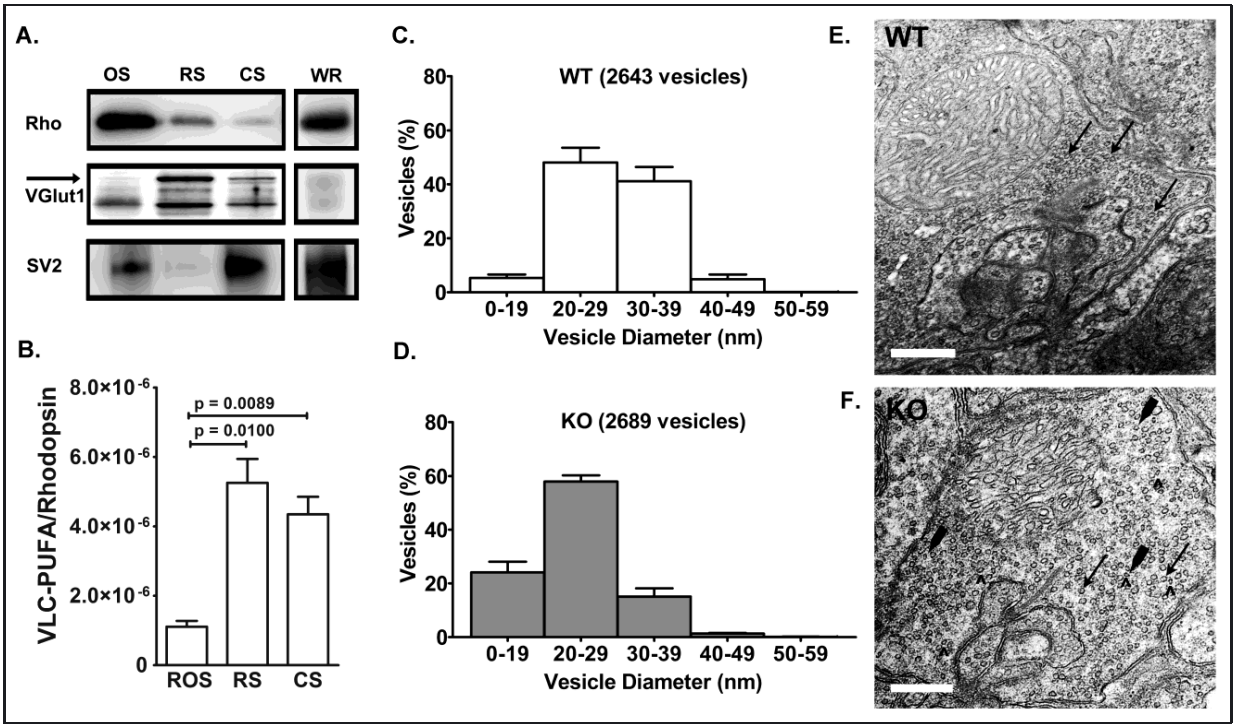

Fig. 2. VLC-PUFAs are enriched in retinal synapses. (A) Representative Western blot of fractionated bovine whole retina (WR) showed that rhodopsin (Rho, 37 kDa) was enriched in rod outer segments (OS), whereas VGlut1 (60 kDa) was localized to the ribbon synaptosome (RS) and synaptic vesicle protein (SV2; 95 kDa) was localized to the conventional synaptosome (CS) fractions. The WR sample was the whole retinal homogenate before centrifugation. (B) Ribbon and conventional synaptosome (RS and CS, respectively) fractions contained VLC-PUFAs that were not derived from OS contamination (n = 4). (C) Vesicles in WT rod terminals were predominately 20 to 39 nm in diameter, whereas the vesicles within the KO mouse terminals (D) were more frequently 20 to 29 nm in diameter. (E) Representative micrograph of a WT rod terminal shows an example of vesicles measuring between 30 and 39 nm (*arrows*). (F) Representative micrograph of a KO rod terminal shows an example of vesicles measuring between 20 to 19 nm (*thick arrowheads*) and 30 to 39 nm (*arrows*). Abnormal vesicles (*empty arrowheads*) appearing "deflated" were frequently observed in the KO mouse spherules. Mice were 12 months of age. *Scale bars*: 500 nm. Data are expressed as mean ± SD. (This research was originally published in *Investigative Ophthalmology and Visual Science*. Bennett *et al.*, (2014). © Association for Research in Vision and Ophthalmology.)

(Redburn and Thomas, 1979). Fractions were confirmed by protein analysis, revealing clean separation of rod outer segments (ROS) from ribbon synapses (RS) from conventional synapses (CS) (Bennett *et al.*, 2014). VLC-PUFA were found in all three membrane preparations. Normalization to rhodopsin, an integral outer segment membrane protein, confirmed that the VLC-PUFA detected within the RS and CS fractions were intrinsic to those membranes and not a result of contamination from the ROS, which are known to be enriched in VLC-PUFA (Figs. 2A and 2B). Lipidomic analysis revealed significant differences in the PC molecular species distribution between the three fractions, indicating the presence of different phospholipid molecular species within each membrane fraction (Tab. 1).

Table 1. Phosphatidylcholine molecular species are different in retinal synaptosomes compared to photoreceptor outer segments.

	RS	CS	ROS
PC34:01, 16:0/18:1*†	12.6 ± 1.2	14.3 ± 0.9	17.3 ± 0.8
PC36:01, 18:0/18:1*†‡	4.9 ± 0.3	6.1 ± 0.4	7.4 ± 0.2
PC38:06, 16:0/22:6*†	8.9 ± 1.0	8.2 ± 0.6	5.9 ± 0.6
PC40:06, 18:0/22:6*†	15.6 ± 2.4	14.8 ± 1.9	10.4 ± 1.4
Σ VLC-PUFA†	4.5 ± 0.3	3.5 ± 0.3	5.4 ± 0.6

PC number of carbons: number of double bonds Σ VLC-PUFA, sum of very long chain polyunsaturated fatty acids; ROS, rod outer segments. * RS *versus* ROS, $p < 0.05$. † CS *versus* ROS, $p < 0.05$. ‡ RS *versus* CS, $p < 0.05$. (This research was originally published in *Investigative Ophthalmology and Visual Science.* Bennett *et al.*, (2014). © Association for Research in Vision and Ophthalmology.)

3 Loss of VLC-PUFA from retinal synapses results in a decrease in both synaptic vesicle diameter and number

Transmission electron microscopy (TEM) was used to evaluate ultrastructural changes within the retinal synapses of *Elovl4* KO and control mice. A randomized blind study revealed that synaptic vesicle diameter was significantly reduced in KO mice at 12 months of age. WT mice had an average vesicle diameter of 29.5 ± 0.93 nm, whereas KO mice had an average vesicle diameter of 24.5 ± 0.62 nm, with the majority measuring less than 29.0 nm (Figs. 2C and 2D). In addition,

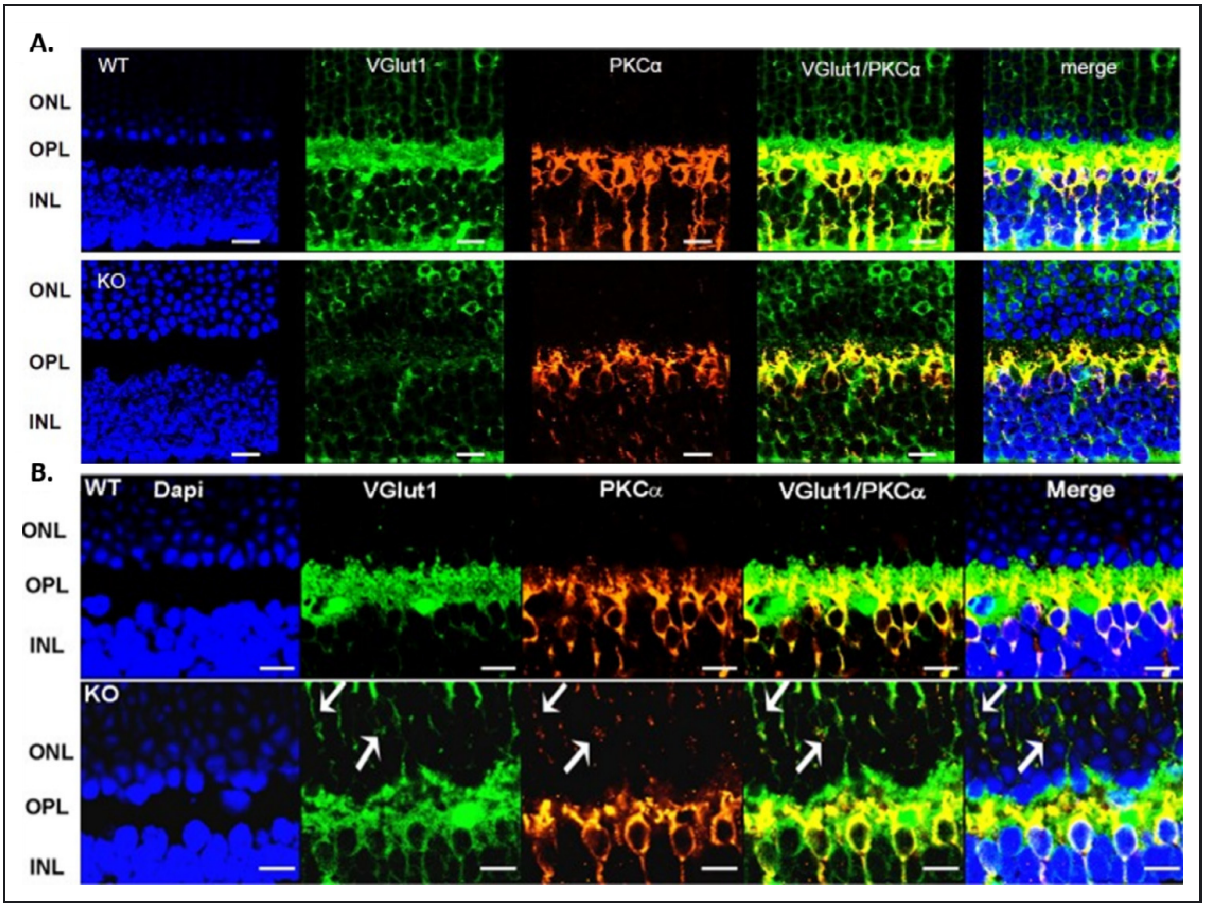

Fig. 3. Reduced VLC-PUFAs caused synaptic terminals to mislocalize in mouse retinas. (A) Glutamatergic vesicles labeled with VGlut1 (*green*) preferentially localized to the OPL in the WT mice but were found predominantly in the ONL of the KO mice. Bipolar dendrites labeled with PKCα (*red*) in the WT and KO mice. *Scale bars*: 20 μm. VLC-PUFA–deficient mice had a loss of photoreceptors and synaptic reorganization. (B) Vesicles labeled with VGlut1 (*green*) were localized with the bipolar cell dendrites labeled with PCK-α (*orange*) in the photoreceptor synaptic layer (OPL) in the WT, but were found in the ONL and OPL in the KO retina. The OPL in the KO retina was disorganized compared to WT with bipolar cell dendrites (*orange*) extending down into the ONL. Similar results were observed from eight different 9-month-old mice per genotype. *Scale bars*: 10 μm. (This research was originally published in *Investigative Ophthalmology and Visual Science.* Bennett *et al.* (2014). © Association for Research in Vision and Ophthalmology.)

the number of tethered presynaptic vesicles (within 40 nm of the synaptic ribbon) was significantly reduced in the KO mice with an average of 3.6 ± 0.2 vesicles/μm of the presynaptic ribbon, while WT mice had an average of 4.7 ± 0.3 vesicles/μm of the presynaptic ribbon (Figs. 2E and 2F).

4 Loss of VLC-PUFA results in synaptic reorganization

Immunohistochemistry performed on WT and KO retinas revealed a notable change in synaptic organization in *Elovl4* KO mice (Figs. 3A and 3B). The rod glutamatergic terminals (marked by VLGUT1 staining) make synaptic connection with bipolar cells (marked by PKC-α staining) within the outer plexiform layer (OPL). In the case of the KO mice, the rod photoreceptor terminals (*green*) appear to withdraw their terminals from the OPL where they should be making connections with the bipolar cell dendrites (*orange*). This results in a loss of VGLUT1 positive terminals in the OPL of KO mice and an increase in PKC-α staining within the outer nuclear layer (ONL) as the bipolar cell dendrites appear to extend downward in an attempt to re-connect with the withdrawn presynaptic terminals. Therefore it is likely that the decreased presynaptic vesicle size and number resulted in decreased synaptic efficiency and drove the subsequent reorganization of the rod terminals and the bipolar dendrites within the OPL.

5 Loss of VLC-PUFA results in rod-mediated functional deficits within the neural retina

Electroretinography (ERG) provides a non-invasive means to assess the electrophysiological responses of the photoreceptor outer segments (a-wave) and the neural retina (b-wave) in response to varying intensities of photostimulation. ERG was performed as described (Bennett *et al.*, 2014) in order to analyze the various stages of the retinal response to light. These

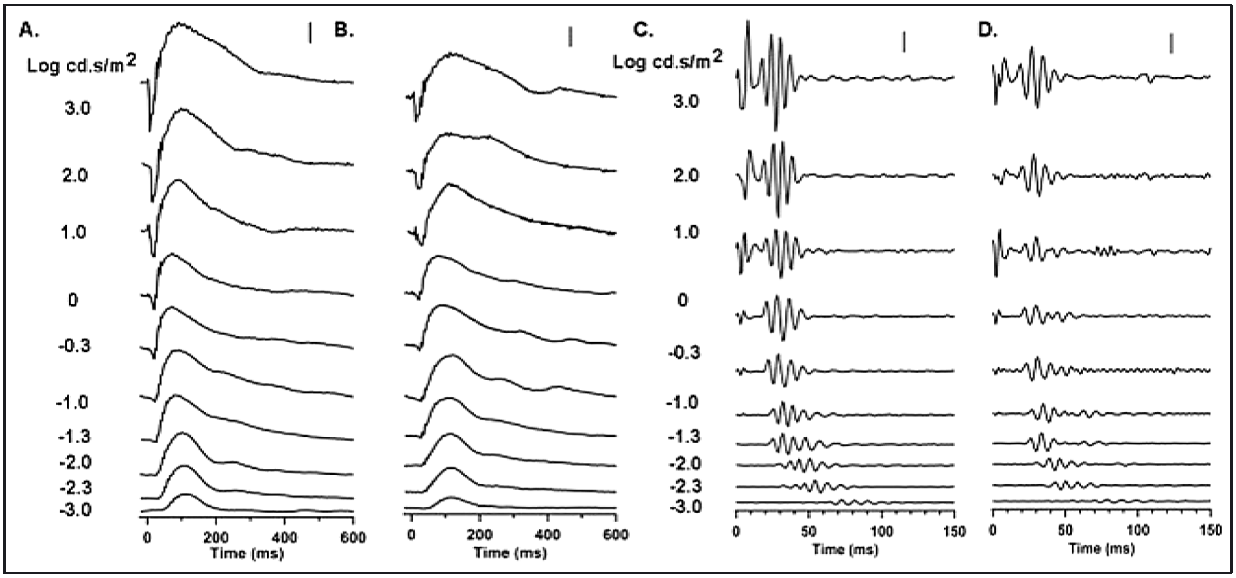

Fig. 4. Rod-mediated function deteriorated in VLC-PUFA–deficient mice. Representative 12-month-old WT (A) responses to increasing light intensities (−3.0 log scot cd·s/m^2 to 3.0 log scot cd·s/m^2) had higher a- and b-wave amplitudes than 9-month-old KO (B) responses. *Vertical bar* at *upper right* in each case is *y*-axis amplitude = 200 μV. (C) WT oscillatory potentials (OPs) had amplitudes higher than the KO (D) OP amplitudes. *Vertical bar* at *upper right* in each case is *y*-axis amplitude = 20 μV. The numbers between the traces in (A, C) are the light intensities (log scot cd·s/m^2) at which the responses were elicited. The latency of the OP responses was not different between the mice. (This research was originally published in *Investigative Ophthalmology and Visual Science*. Bennett *et al.* (2014). © Association for Research in Vision and Ophthalmology.)

studies revealed that the outer segment-mediated a-wave was significantly reduced in the KO mice compared to WT mice. This loss of a-wave response could be explained by the loss of rod photoreceptor cells. In addition, the b-wave response induced by the photoreceptor pre-synaptic terminals and mediated by the neural retina was also significantly reduced in KO mice compared to WT (Figs. 4A and 4B). This reduction in b-wave amplitude, however, was greater than predicted from the loss or rod photoreceptor cells and represented specific changes in the retinal synapses in the KO mice. Using a Butterworth filter (30 and 80 Hz) to remove a- and b-wave contamination allowed for the isolation of oscillatory potentials (OPs), which are mediated by the synaptic feedback responses of amacrine, horizontal, and bipolar cells to the initial rod photoresponse (Wachtmeister, 1998). OP amplitudes were significantly decreased in KO mice compared to WT mice, suggesting a decrease in synaptic efficiency within the neural retina following depletion of VLC-PUFA (Figs. 4C and 4D).

6 Deficits in synaptic transmission due to the absence of vlc-pufa are not due to deficits in pre-synaptic calcium currents or post-synaptic glutamatergic currents

Whole-cell patch clamp recordings were used to evaluate the amplitude and voltage dependence of pre-synaptic rod photoreceptor inward calcium currents (I_{Ca}) as well as glutamate-mediated post-synaptic currents in retinal slices from both WT and KO mice. Recordings were performed under standard conditions as described previously (Bennett *et al.*, 2014; Van Hook and Thoreson, 2013). There was no significant difference in I_{Ca} between WT and KO mice, indicating that loss of pre-synaptic I_{Ca} are not responsible for any decreases in synaptic transmission in KO mice (Figs. 5A–5C). Post-synaptic glutamatergic currents mediated by mGluR6 were evaluated by measuring responses to the mGluR6 antagonist CPPG applied in the presence of the metabotropic glutamate receptor group 3-selective agonist L-2-amino-4-phosphonobutyric acid (L-AP4). Rod bipolar cells were voltage clamped at −60 mV and responses were evoked by transient and localized CPPG application. Inward rod bipolar cell mediated currents were measured and no significant differences were detected between WT and KO mice, indicating that changes in the b-wave were not mediated by dysregulation of post-synaptic glutamate receptor currents (Figs. 5D–5F). A lack of significant differences between WT and KO mice in both pre-synaptic I_{Ca} and post-synaptic rod bipolar cell glutamate receptor currents indicates that the decrease in synaptic transmission is most likely due to deficits in pre-synaptic release downstream of I_{Ca}, but upstream of post-synaptic metabotropic glutamate receptor responses. This is consistent with the possibility that the deficit in the b-wave arises from decreases in presynaptic release of glutamate, perhaps due to a small number of pre-synaptic vesicles or a decrease in vesicle size.

7 Decreases in B-wave neural retina responses correlate with decreases in pre-synaptic release of glutamate

The diameters of synaptic vesicles from KO mice were significantly smaller than those from WT mice, 24.5 nm *vs.*

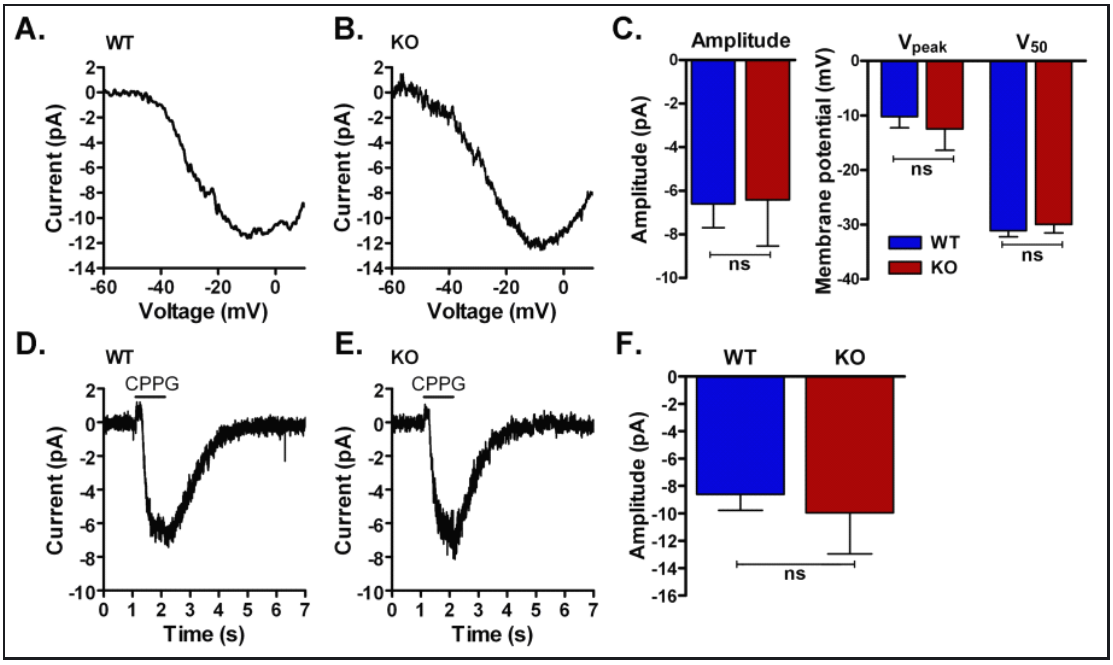

Fig. 5. Rod calcium currents (I_{Ca}) and rod bipolar cell (RBC) glutamate receptor signaling were similar between 12-month-old WT and KO mice. (A) Representative I_{Ca} recorded with a voltage ramp (−90 to +60, 0.5 mV/ms) in a rod from a WT retina. The displayed trace is an average of two traces from a single cell. (B) I_{Ca} from a KO rod. The displayed trace is an average of three traces from a single cell. (C) *Left*: group data, showing that the I_{Ca} amplitude was similar in WT and KO rods. Likewise, the voltage dependence, as indicated by the peak voltage (V_{peak}) and voltage of half-maximal activation (V_{50}), was similar in rods from WT and KO mouse retinas. (D) Response of an RBC from a WT retina to a 1-second puff of CPPG (600 μM) in the presence of L-AP4 (4 μM). The RBC was voltage clamped at −60 mV, and the displayed trace is an average of five traces. (E) Response of an RBC from a KO retina. The displayed trace is an average of five traces. (F) Amplitudes of RBC responses to CPPG puffs were similar in WT and *Elovl4* KO mouse retinas. Data are mean ± SEM. ns, not significant. (This research was originally published in *Investigative Ophthalmology and Visual Science*. Bennett *et al.* (2014). © Association for Research in Vision and Ophthalmology.)

29.5 nm (Figs. 2C and 2D). Because volume scales with the cube of radius, this relatively small change in diameter would result in a reduction in volume (and thus glutamate content) of ~57% (43% of control). This reduction in glutamate content could explain the roughly 50% decrease in b-wave amplitude in KO mice.

8 Discussion

Our studies demonstrate a clear role for ELOVL4 in supporting the structural and functional integrity of neuronal synapses within the mammalian retina. VLC-PUFA are not exclusively expressed in photoreceptor outer segments as was previously thought, but rather are present within both the large ribbon synapses made up of the photoreceptor and bipolar cells as well as the smaller conventional synapses utilized by the rest of the neural retina. The depletion of these very long chain fatty acids clearly provoked changes in the membrane structure of presynaptic photoreceptor terminals, causing them to withdraw into the ONL away from the bipolar cell dendrites, creating a larger distance for glutamate to diffuse before reaching its post-synaptic target. This retraction of pre-synaptic terminals from their post-synaptic targets, combined with a decrease in synaptic vesicle diameter and number, results in less glutamate being released and translates into a gross dysregulation of synaptic efficiency, which can be measured directly by decreases in the electrophysiological responses of the scotopic system. This dysregulation cannot be accounted for by changes in inward pre-synaptic I_{Ca}, which are necessary for synaptic vesicle docking and release (DeLorenzo and Freedman, 1978; Katz and Miledi, 1967) or by changes in post-synaptic glutamate receptor-mediated currents. This further supports the idea that the changes measured within the scotopic system are mediated by the decrease in pre-synaptic vesicle diameter and number, translating to a smaller pool of releasable vesicles as well as a decrease in the quantal size of individual vesicles. The reduction in vesicle diameter results in an average volume reduction of 57%, which correlates with a decrease in scotopic b-wave responses of ~50% at higher stimulus intensities. It is important to note that these studies were conducted on 12-month-old mice and that this is an age-dependent phenotype where over time the reduction of these VLC-products results in retinal degeneration, synaptic remodeling, and dysregulation of synaptic function.

In an earlier publication from our group, (Brush *et al.*, 2010), we found very long chain saturated fatty acids (sum of 26:0 + 28:0 + 30:0) in the neutral sphingolipids of the rat and bovine retina, as well as in bovine ROS. Since ELOVL4 is responsible for the synthesis of all very-long chain fatty acids (≥ C26) regardless of their degree of unsaturation, another possible scenario is that these very long chain saturated fatty acids, which exist as components of sphingolipid molecules,

are providing a significant level of structural support for synaptic membrane size, while the very-long chain polyunsaturated fatty acids, which exist as components of phosphatidylcholine molecules, are providing a significant level of structural support for synaptic membrane morphology and fluidity. The longer the fatty acid chain, the more dynamic its influence can be on the structural and biophysical properties of a membrane. The biophysical properties of these two types of VLC-FA are very different, so it is possible that their ratios must be carefully balanced to achieve the proper size and curvature of a synaptic vesicle membrane. The loss of the VLC-PUFA could explain the significant changes in synaptic vesicle morphology, such as the lack of curvature, while the loss of the VLC-SFA could explain the significant reduction in synaptic vesicle size, as both ultrastructural changes were found in *Elovl4* KO mice (Bennett *et al.*, 2014).

Acknowledgements. We thank Nicole A. Rocha for writing the program which allowed us to extract and analyze oscillatory potentials. We thank members of the Dean Bok laboratory (University of California-Los Angeles, Los Angeles, CA, USA) for their help in the perfusion experiments and Shelby Wilkinson for technical assistance. We thank Dianna Johnson (University of Tennessee Health Science Center, Memphis, TN, USA) for valuable discussions related to retinal synapses. Supported by National Institutes of Health Grants EY00871, EY04149, P30EY021725, and P20RR017703 (REA) and EY10542 (WBT); Foundation Fighting Blindness (REA); Reynolds Oklahoma Aging Center (REA); Research to Prevent Blindness (Dean McGee Eye Institute and University of Nebraska Medical Center); Fight for Sight (MJVH); and Senior Scientific Investigator Award from Research to Prevent Blindness (WBT).

Disclosure. B.R. Hopiavuori, None; L.D. Bennett, None; R.S. Brush, None; M.J. Van Hook, None; W.B. Thoreson, None; R.E. Anderson, None

References

Agbaga MP, Brush RS, Mandal MN, Henry K, Elliott MH, Anderson RE. 2008. Role of Stargardt-3 macular dystrophy protein (ELOVL4) in the biosynthesis of very long chain fatty acids. *Proc. Natl. Acad. Sci. USA* 105: 12843–12848.

Agbaga MP, Mandal MN, Anderson RE. 2010. Retinal very long-chain PUFAs: new insights from studies on ELOVL4 protein. *J. Lipid. Res.* 51: 1624–1642.

Agbaga MP, Tam BM, Wong JS, Yang LL, Anderson RE, Moritz OL. 2014. Mutant ELOVL4 that causes autosomal dominant stargardt-3 macular dystrophy is misrouted to rod outer segment disks. *Invest. Ophthalmol. Vis. Sci.* 55: 3669–3680.

Aveldano MI. 1987. A novel group of very long chain polyenoic fatty acids in dipolyunsaturated phosphatidylcholines from vertebrate retina. *J. Biol. Chem.* 262: 1172–1179.

Barabas P, Liu A, Xing W, *et al.* 2013. Role of ELOVL4 and very long-chain polyunsaturated fatty acids in mouse models of Stargardt type 3 retinal degeneration. *Proc. Natl. Acad. Sci. USA* 110: 5181–5186.

Bennett LD, Hopiavuori BR, Brush RS, *et al.* 2014. Examination of VLC-PUFA-deficient photoreceptor terminals. *Invest. Ophthalmol. Vis. Sci*. doi: 10.1167/iovs.14-13997

Brush RS, Tran JT, Henry KR, McClellan ME, Elliott MH, Mandal MN. 2010. Retinal sphingolipids and their very-long-chain fatty acid-containing species. *Invest. Ophthalmol. Vis. Sci.* 51: 4422–4431.

DeLorenzo RJ, Freedman SD. 1978. Calcium dependent neurotransmitter release and protein phosphorylation in synaptic vesicles. *Biochem. Biophys. Res. Commun.* 80: 183–192.

Donoso LA, Frost AT, Stone EM, *et al.* 2001. Autosomal dominant Stargardt-like macular dystrophy: founder effect and reassessment of genetic heterogeneity. *Arch. Ophthalmol.* 119: 564–570.

Edwards AO, Donoso LA, Ritter R, 3rd. 2001. A novel gene for autosomal dominant Stargardt-like macular dystrophy with homology to the SUR4 protein family. *Invest. Ophthalmol. Vis. Sci.* 42: 2652–2663.

Griesinger, IB, Sieving, PA, and Ayyagari, R. 2000. Autosomal dominant macular atrophy at 6q14 excludes CORD7 and MCDR1/PBCRA loci. *Invest. Ophthalmol. Vis. Sci.* 41: 248–255.

Harkewicz R, Du H, Tong Z, *et al.* 2012. Essential role of ELOVL4 protein in very long chain fatty acid synthesis and retinal function. *J. Biol. Chem.* 287: 11469–11480.

Katz B, Miledi R. 1967. The timing of calcium action during neuromuscular transmission. *J. Physiol.* 189: 535–544.

Kniazeva M, Chiang MF, Morgan B, Anduze AL, Zack DJ, Han M, Zhang K. 1999. A new locus for autosomal dominant stargardt-like disease maps to chromosome 4. *Am. J. Hum. Genet.* 64: 1394–1399.

Logan S, Agbaga MP, Chan MD, *et al.* 2013. Deciphering mutant ELOVL4 activity in autosomal-dominant Stargardt macular dystrophy. *Proc. Natl. Acad. Sci. USA* 110: 5446–5451.

Logan S, Agbaga MP, Chan MD, Brush RS, Anderson RE. 2014. Endoplasmic reticulum microenvironment and conserved histidines govern ELOVL4 fatty acid elongase activity. *J. Lipid. Res.* 55: 698–708.

Poulos A. 1995. Very long chain fatty acids in higher animals–a review. *Lipids* 30: 1–14.

Poulos A, Johnson DW, Beckman K, White IG, Easton C. 1987. Occurrence of unusual molecular species of sphingomyelin containing 28-34-carbon polyenoic fatty acids in ram spermatozoa. *Biochem. J.* 248: 961–964.

Redburn DA, Thomas TN. 1979. Isolation of synaptosomal fractions from rabbit retina. *J. Neurosci. Methods* 1: 235–242.

Van Hook MJ, Thoreson WB. 2013. Simultaneous whole cell recordings from photoreceptors and second-order neurons in an amphibian retinal slice preparation. *J. Vis. Exp.* e50007.

Vasireddy V, Uchida Y, Salem N, Jr, *et al.* 2007. Loss of functional ELOVL4 depletes very long-chain fatty acids (>or = C28) and the unique omega-O-acylceramides in skin leading to neonatal death. *Hum. Mol. Genet.* 16: 471–482.

Wachtmeister L. 1998. Oscillatory potentials in the retina: what do they reveal. *Prog. Retin Eye Res.* 17: 485–521.

Zhang K, Kniazeva M, Han M, *et al.* 2001. A 5-bp deletion in ELOVL4 is associated with two related forms of autosomal dominant macular dystrophy. *Nat. Genet.* 27: 89–93.

Cite this article as: Blake R. Hopiavuori, Lea D. Bennett, Richard S. Brush, Matthew J. Van Hook, Wallace B. Thoreson, Robert E. Anderson. Very long-chain fatty acids support synaptic structure and function in the mammalian retina. OCL 2016, 23(1) D113.